

Compact Stellarators as Reactors

J. F. Lyon 1), P. M. Valanju 2), M. C. Zarnstorff 3), S. P. Hirshman 1), D. A. Spong 1),
D. J. Strickler 1), A. S. Ware 4), D. E. Williamson 1)

- 1) Oak Ridge National Laboratory, Oak Ridge, TN, U.S.A.
- 2) University of Texas at Austin, Austin, TX, U.S.A.
- 3) Princeton Plasma Physics Laboratory, Princeton, NJ, U.S.A.
- 4) University of Montana, Missoula, MT, U.S.A.

e-mail contact of main author: lyonjf@fed.ornl.gov

Abstract. Two types of compact stellarators are examined as reactors: two- and three-field-period ($M = 2$ and 3) quasi-axisymmetric devices with volume-average $\langle\beta\rangle = 4$ -5% and $M = 2$ and 3 quasi-poloidal devices with $\langle\beta\rangle = 10$ -15%. These low-aspect-ratio stellarator-tokamak hybrids differ from conventional stellarators in their use of the plasma-generated bootstrap current to supplement the poloidal field from external coils. Using the ARIES-AT model with $B_{\max} = 12$ T on the coils gives Compact Stellarator reactors with $R = 7.3$ -8.2 m, a factor of 2-3 smaller R than other stellarator reactors for the same assumptions, and neutron wall loadings up to 3.7 MW m⁻².

1. Compact Stellarator Reactor Configurations

Compact stellarators [1] are stellarator-tokamak hybrids with plasma aspect ratios $A_p = R/a_p < 5$ in which the poloidal field is created by both currents in external windings and the plasma bootstrap current. These devices may combine the best features of tokamaks (moderate A_p , good confinement, and high $\langle\beta\rangle$) and currentless stellarators (steady-state operation without external current drive or disruptions, stability against external kinks and vertical displacement events without a close conducting wall or active feedback systems, and low recirculating power in a reactor). The earlier $R = 14$ m Stellarator Power Plant Study (SPPS) reactor [2] was calculated to be cost competitive with the $R = 6$ m ARIES-IV and $R = 5.5$ m ARIES-RS tokamak reactors with higher wall power density largely due to SPPS's low recirculated power [3]. A more compact stellarator reactor could retain the cost savings associated with the low recirculated power of the SPPS reactor, but with smaller size and higher wall power density (hence lower cost of electricity) than the SPPS reactor.

Two types of low- A_p compact stellarators were examined as reactors: quasi-axisymmetric (QA) cases [4] with $\langle\beta\rangle = 4$ -5% and quasi-poloidal (QP) cases [5] with $\langle\beta\rangle = 10$ -15%. Figure 1 shows the last closed flux surface and the $|B|$ contours on that surface for three compact stellarator examples; here purple indicates the lowest $|B|$ value and red the highest.

The coils that create these configurations are characterized by $A_\Delta = R/\Delta$ and B_{\max}/B_0 where Δ is the minimum distance between the plasma edge and the centerline of the coils for a given R , and B_{\max} is the maximum field on the coils. These ratios depend on the specific coil design and are important because the minimum reactor size is set by $R_{\min} = A_\Delta(d + ct/2)$ where d is

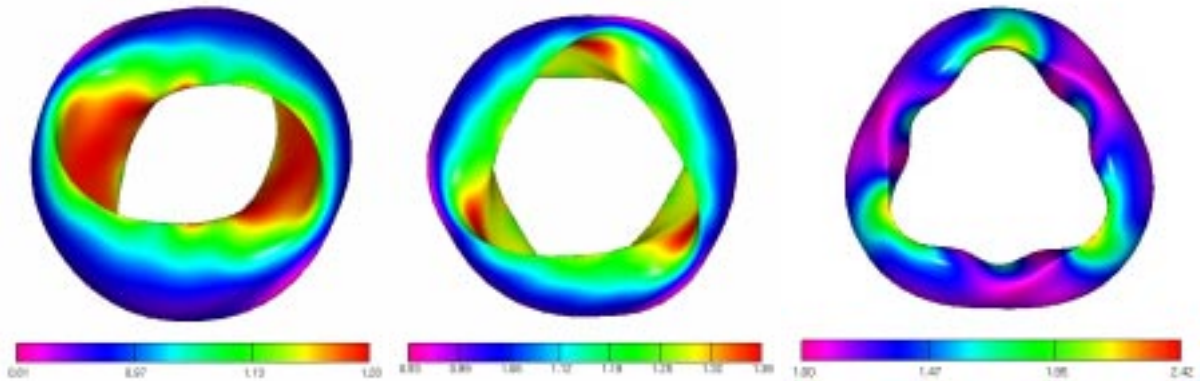


Fig. 1. (a) $M = 2$ $A_p = 2.95$ QA. (b) $M = 3$ $A_p = 4.4$ QA. (c) $M = 3$ $A_p = 3.7$ QP.

the limiting (inboard) space needed for the plasma-wall distance, first wall, blanket, shield, vacuum vessel, and assembly gaps. The half radial depth of the modular coils is given by

$$ct/2 = A_{\Delta} B_0 / (16 N_{\text{coil}} j_{\text{coil}} k) [1 + \{1 + 32 N_{\text{coil}} j_{\text{coil}} k d / (A_{\Delta} B_0)\}^{1/2}]$$

where N_{coil} is the number of coils, j_{coil} is the current density averaged over the coil cross section in kA cm^{-2} , and k is the ratio of toroidal width to radial depth of the coils. A 20-cm thick cryostat surrounds the reactor core. The value assumed for d is 1.12 m, similar to that for ARIES-AT [6]; the value on the outboard side is 1.30 m. The other reference reactor assumptions are also similar to those for ARIES-AT; e.g., a thermal conversion efficiency $\eta = 59\%$ and $B_{\text{max}} = 12$ T whereas the SPPS reactor had $\eta = 46\%$ and $B_{\text{max}} = 16$ T.

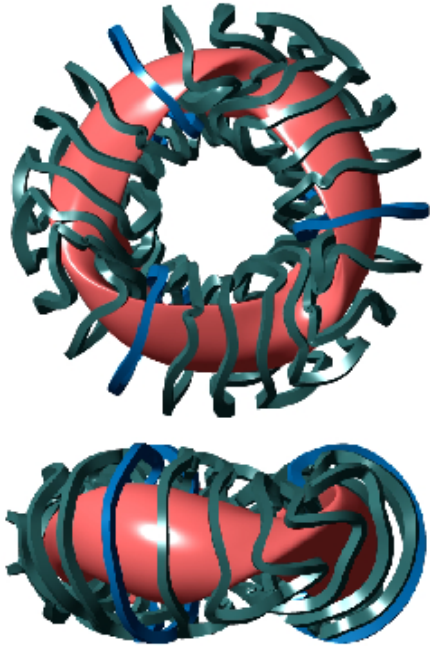


Fig. 2. A modular coil set for the QA plasma configuration shown in Fig. 1(b).

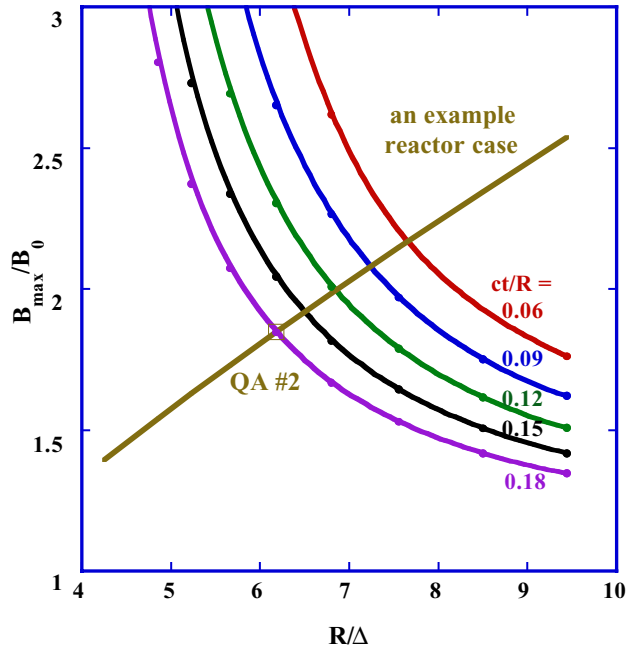


Fig. 3. Variation of B_{max}/B_0 with R/Δ for the QA plasma configuration shown in Fig. 1(b).

2. Results for the Scaling Model

Figure 2 shows a particular modular coil set for the plasma configuration shown in Fig. 1(b). Rather than calculating actual coils for a large number of possible coil-plasma distances and coil cross sections, an approximate model was used for a scaling study. The NESCOIL code [7] was used to calculate B_{max}/B_0 at a distance $ct/2$ radially in from a current sheet (at a distance Δ from the plasma edge) that reproduced the last closed flux surface. The value of B_{max}/B_0 was increased by 15% to simulate effects due to a smaller number of coils from experience in the SPPS study. Figure 3 shows the tradeoff between minimizing B_{max}/B_0 , which increases the field in the plasma for a given B_{max} on the coils, and maximizing Δ to allow a smaller R for a reactor with a given d , for the QA case shown in Fig. 1(b). Similar calculations were done for the QA case in Fig. 1(a) and the QA values were used for similar QP cases. Because the fusion power P_{fusion} (and hence the net electric power generated, P_{electric}) $\propto \beta^2 B_0^4 V_{\text{plasma}}$, the value of B_{max}/B_0 needed for a given P_{electric} and d is proportional to $(R/\Delta)^{3/4}$, as indicated by the “example reactor” line in Fig. 3.

Using this model, the minimum value for R was calculated for $M = 2$ and 3 QA and QP reactors for each ct/R value subject to several constraints: $P_{\text{electric}} = 1$ GW, $\Gamma_n \leq 4$ MW m^{-2} , a plasma-coil distance ≥ 1.11 m, $j_{\text{coil}} \leq 3$ kA cm^{-2} , $H-95 \leq 3.5$, $\langle n \rangle / n_{\text{Sudo}} \leq 1$, and $\langle \beta \rangle \leq 5\%$. Here $H-95 = \tau_E / \tau_E^{\text{ISS95}}$ where $\tau_E^{\text{ISS95}} = 0.79 a_p^{2.21} R^{0.65} P^{-0.59} n^{0.51} B^{0.83} t^{-0.4}$ [8] and $n_{\text{Sudo}} = (1/4)[PB/Ra^2]^{1/2}$ [9] with R and a_p in m, B in T, n in 10^{20} m^{-3} , and P in MW. The value for Γ_n is an important figure of merit for reactor economics because it relates to the power generated

per unit wall area and the costs of the main reactor core elements (blankets, shield, and coils) are proportional to the wall area. Table 1 shows the results for the two QA and QP cases. The minimum values for R and H-95 are obtained with $\langle n \rangle / n_{\text{Sudo}} = 1$.

Table 1. Scaled 1-GW Compact Stellarator Reactors with $B_{\text{max}} = 12$ T, $\langle \beta \rangle \leq \beta_{\text{limit}}$, H-95 ≤ 5 .

	QA#1	QA#2	QP#1	QP#2
Plasma aspect ratio R/a_p	2.96	4.4	2.70	3.70
Volume average β limit $\langle \beta \rangle_{\text{limit}}$ (%)	4	4.1	10	15
Average major radius R (m)	8.22	9.93	7.34	7.84
Average plasma radius a_p (m)	2.78	2.26	2.72	2.12
Plasma volume V_{plasma} (m ³)	1250	1000	1040	690
On-axis field B_0 (T)	5.41	5.65	5.23	5.03
$\tau_E/\tau_E^{\text{ISS95}}$ multiplier H-95	2.65	2.62	3.61	4.42
Volume average beta $\langle \beta \rangle$ (%)	4	4.1	4.6	6.2
Energy confinement time τ_E (s)	2.69	2.41	2.49	2.01
Vol.-average density $\langle n \rangle$ (10 ²⁰ m ⁻³)	1.31	1.50	1.40	1.70
Density-aver. temperature $\langle T \rangle$ (keV)	11.1	10.8	11.3	11.5
Neutron wall load Γ_n (MW m⁻²)	1.34	1.37	1.54	1.85

The higher $\langle \beta \rangle$ allowed for the QP configurations requires higher values for H-95. The higher $\langle \beta \rangle$ also allows reducing B_{max} , which leads to smaller R and higher Γ_n . For the QP#1 case, reducing B_{max} from 12 T to 8.5 T reduced R from 7.34 m (with H-95 = 3.6 and $\langle \beta \rangle = 4.6\%$) to $R = 7.09$ m (with H-95 = 5.4 and $\langle \beta \rangle = 9.7\%$) and increased Γ_n from 1.37 MW m⁻² to 1.65 MW m⁻². Increasing β_{limit} to 5% for the QA configurations also led to smaller values for R : $R = 7.08$ m for QA#1 with H-95 = 2.90 and $\Gamma_n = 1.81$ MW m⁻²; and $R = 8.80$ m for QA#2 [Fig. 1(b)] with H-95 = 2.82 and $\Gamma_n = 1.74$ MW m⁻².

Table 2 shows the same analysis for $P_{\text{electric}} = 2$ GW. The values for B_0 are unchanged because B_{max} was assumed to be 12 T at 1 GW and 2 GW. For the QA cases, the values for τ_E , $\langle n \rangle$ and $\langle T \rangle$ are unchanged because the beta limit had already been reached at 1 GW. Because $P_{\text{electric}} \propto \beta^2 B_0^4 V_{\text{plasma}}$ and β and B_0 do not increase, the plasma volume doubles to produce twice the power, so R and Γ_n increase by a factor of $2^{1/3} = 1.26$. H-95 decreases by a factor 1.29 to accommodate the increased $a_p^{2.21} R^{0.65} P^{-0.59}$ factor in τ_E^{ISS95} . For the QP cases, the beta limit is not reached at 2 GW, so the reactor size is unchanged; β increases by a factor $2^{1/2}$ to produce twice the power, Γ_n doubles, and τ_E decreases by a factor $2^{1/2}$ because $\tau_E \propto$

Table 2. Scaled 2-GW Compact Stellarator Reactors with $B_{\text{max}} = 12$ T, $\langle \beta \rangle \leq \beta_{\text{limit}}$, H-95 ≤ 4 .

	QA#1	QA#2	QP#1	QP#2
Average major radius R (m)	10.35	12.51	7.34	7.85
Average plasma radius a_p (m)	3.50	2.84	2.72	2.12
Plasma volume V_{plasma} (m ³)	2500	2000	1070	700
$\tau_E/\tau_E^{\text{ISS95}}$ multiplier H-95	2.07	2.04	3.56	3.94
Volume average beta $\langle \beta \rangle$ (%)	4	4.1	6.5	8.75
Energy confinement time τ_E (s)	2.69	2.41	1.76	1.42
Vol.-ave. density $\langle n \rangle$ (10 ²⁰ m ⁻³)	1.31	1.50	1.62	2.40
Density-aver. temperature $\langle T \rangle$ (keV)	11.1	10.8	13.7	11.5
Neutron wall load Γ_n (MW m⁻²)	1.69	1.72	3.07	3.68

$\beta/P_{\text{electric}}$. The value for $n_{\text{Sudo}} \propto P_{\text{electric}}^{1/2}$ increases by $2^{1/2}$ and $\langle T \rangle \propto P_{\text{electric}} \tau_E / \langle n \rangle$, so $\langle n \rangle$ should increase by a factor of $2^{1/2}$ and $\langle T \rangle$ should not change. This occurs for the QP#2 case where $\langle n \rangle / n_{\text{Sudo}} = 1$, but not for the QP#1 case where $\langle n \rangle / n_{\text{Sudo}}$ is only 0.82. The value needed for H-95 only decreases by 1.4% for the QP#1 case and by 10.9% for the QP#2 case. Increasing the allowed value for $\langle n \rangle$ to $2 \times n_{\text{Sudo}}$ (as in LHD) did not decrease R_{min} for $B_{\text{max}} = 12$ T but decreased the required H-95 multiplier by a factor of ~ 1.3 . Increasing B_{max} to 16 T, as for ARIES-IV, increased R_{min} for the QP reactors by only 25 cm, but decreased $\langle \beta \rangle$ by a factor of 1.86 and H-95 to 2.41 for QP#1 and 2.96 for QP#2. This had a much larger effect on the QA reactors, which were beta limited at $\approx 4\%$ in Table 2; R_{min} dropped to 7.28 m for the QA#1 case and 9.15 m for QA#2 case, close to that obtained for the QP cases.

The same assumptions were used with the plasma and coil configurations corresponding to the W7-X based HSR [10], the LHD based MHR-S [11], and SPPS reactors for comparison with these reactor studies. The modified HSR* had $R = 17.4$ m (instead of 22 m because B_{max} was increased from 10.6 T to 12 T), H-95 = 3.06, $\langle \beta \rangle = 4.9\%$, and $\Gamma_n = 1.24$ MW m⁻². The modified MHR-S* had $R = 18.6$ m (instead of 16.5 m because of the ARIES-AT blanket and shield assumptions), H-95 = 2.87, $\langle \beta \rangle = 5\%$, and $\Gamma_n = 0.62$ MW m⁻². The modified SPPS* had $R = 20.8$ m (instead of 14.0 m because B_{max} was decreased from 16 T to 12 T), H-95 = 3.13, $\langle \beta \rangle = 5\%$, and $\Gamma_n = 0.60$ MW m⁻². For the same modeling assumptions, the compact stellarator configurations lead to reactors with a factor of 2 to 3 smaller major radius and a factor of 1.4 to 3 higher wall power loading.

3. Results for Two Reference Compact Stellarator Reactor Cases

Figure 4 shows a POPCON plot of the operating space ($\langle n \rangle$ and $\langle T \rangle$) for a QA#1 reactor with $R = 7.1$ m and $B_0 = 5.4$ T. The numbers label contours of constant auxiliary heating power in MW, “0” indicates ignition, and the curves indicate constant levels of $\langle \beta \rangle$, P_{electric} , and the Sudo density “limit”. The red dot marks the thermally stable 1-GW_{electric} operating point. The reference reactor assumptions are $A_{\Delta} = 4.84$, $B_{\text{max}} = 12$ T, ARIES-AT inboard blanket and shield, and $P_{\text{fusion}} = 1.69$ GW [$P_{\text{electric}} = 1$ GW (net)]. The reference plasma assumptions are broad ARIES-AT density profiles with $n_e \leq n_{\text{Sudo}}$, peaked ARIES-AT temperature profiles, $\tau_{\text{He}}/\tau_E = 6$, and an alpha-particle energy loss fraction = 0.1. The plasma parameters at the operating point are $\langle n \rangle = 1.7 \times 10^{20}$ m⁻³, $\langle T \rangle = 9.3$ keV, $\langle \beta \rangle = 4.04\%$, H-95 = 2.90, $n_{\text{DT}}/n_e = 0.82$, $n_{\text{He}}/n_e = 5.9\%$, and $Z_{\text{eff}} = 1.48$. The saddle point in Fig. 4 determines the startup power required to reach ignition. Plasma parameters at the saddle point are $\langle n \rangle = 1.1 \times 10^{20}$ m⁻³, $\langle T \rangle = 5.4$ keV, $\langle \beta \rangle = 1.5\%$, and $P_{\text{aux}} = 20$ MW. The H-95 confinement improvement

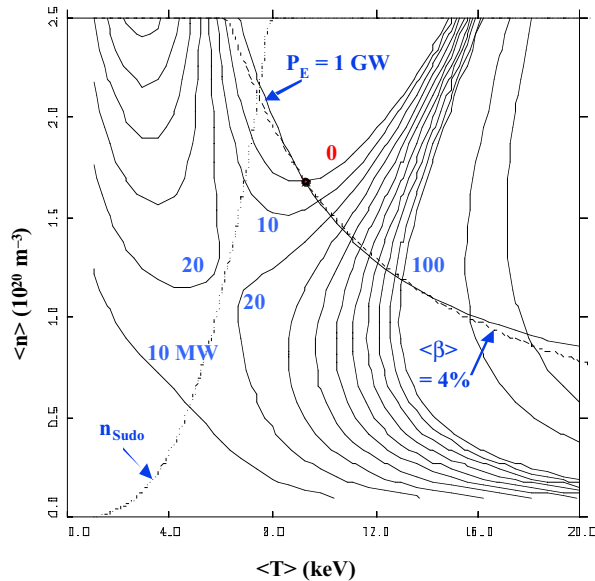


Fig. 4. Operating space for a QA#1 reactor.

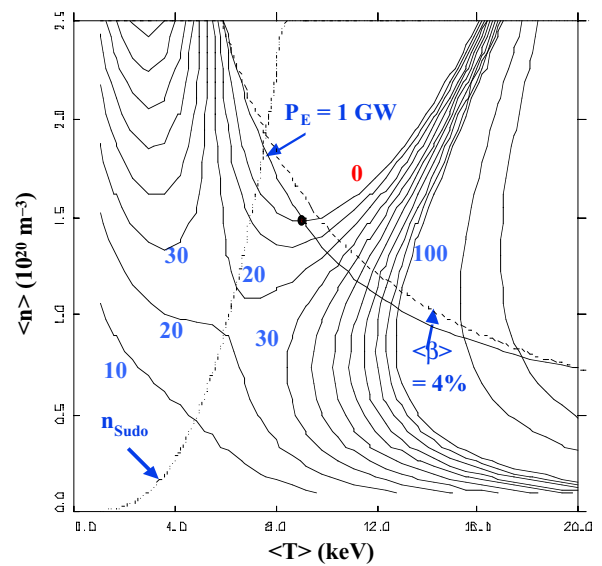


Fig. 5. Operating space for a 1-GW QP#1 reactor.

required increases if the alpha-particle power lost increases. The allowable alpha-particle energy loss varies from 5% at H-95 = 2.8 to 50 % at H-95 = 4.6

Figure 6 shows a POPCON plot for a 1-GW QP#1 reactor with $R = 7.3$ m and $B_0 = 5.2$ T. The plasma parameters at the operating point are $\langle n \rangle = 1.5 \times 10^{20} \text{ m}^{-3}$, $\langle T \rangle = 9.1$ keV, $\langle \beta \rangle = 3.74\%$, H-95 = 2.95, $n_{DT}/n_e = 0.82$, $n_{He}/n_e = 5.8\%$, and $Z_{\text{eff}} = 1.48$. The plasma parameters at the saddle point are $\langle n \rangle = 0.9 \times 10^{20} \text{ m}^{-3}$, $\langle T \rangle = 5.4$ keV, $\langle \beta \rangle = 1.4 \%$, and $P_{\text{aux}} = 20$ MW.

The same reactor could produce 2 GW as shown in Fig. 7 where the plasma parameters at the operating point have increased to

$\langle n \rangle = 2.0 \times 10^{20} \text{ m}^{-3}$, $\langle T \rangle = 9.3$ keV, $\langle \beta \rangle = 5.28\%$, for H-95 = 2.65. The plasma parameters at the saddle point are $\langle n \rangle = 1.3 \times 10^{20} \text{ m}^{-3}$, $\langle T \rangle = 5.4$ keV, $\langle \beta \rangle = 1.4 \%$, and $P_{\text{aux}} = 39$ MW. The higher beta limit also allows decreasing the magnetic field on the coils. Reducing B_{max} from 12 T to 8.5 T requires increasing H-95 from 2.95 to 4.1 for 1-GW operation. The values of $\langle n \rangle$ and $\langle T \rangle$ at the saddle point and the operating point are unchanged, but $\langle \beta \rangle$ increases to 3.1% at the saddle point and 8.4% at the operating point.

4. Conclusions

Both the quasi-axisymmetric and quasi-poloidal configurations have the potential for a more attractive stellarator reactor. Using the ARIES-AT model with $B_{\text{max}} = 12$ T on the coils gives compact stellarator reactors with $R = 7.3$ -8.2 m, a factor of 2-3 smaller in R than other stellarator reactors for the same assumptions. The two-field-period configurations lead to smaller reactors because of their lower plasma aspect ratios and smaller values for R/Δ . The QA configurations generally require less confinement improvement, and the QP configurations are better suited for higher power reactors or lower magnetic field on the coils.

Acknowledgments

This research was supported by the U.S. Dept. of Energy under contract DE-AC05-00OR22725 with UT-Battelle, LLC, and contract DE-AC020-76-CHO3073 with Princeton Plasma Physics Laboratory. The authors acknowledge guidance from F. Najmabadi on the ARIES-AT assumptions relevant for this study and discussions with the NCSX and QOS groups on magnetic configuration and coil design issues.

References

- [1] NEILSON, G.H. et al., *Phys. Plasmas* **7** (2000) 1911.
- [2] Stellarator Power Plant Study, UCSD-ENG-004 (1997).
- [3] LYON, J.F., et al., Plasma Physics and Controlled Nuclear Fusion Research 1994, Seville 1994, Vol. 2, 655 (IAEA Vienna 1985); also LYON, J.F., et al., *Fusion Engineering and Design* **25** (1994) 85.
- [4] ZARNSTORFF, M.C. et al., this conference.
- [5] SPONG, D.A. et al., this conference.
- [6] NAJMABADI, F. et al., this conference.
- [7] MERKEL, P., *Nucl. Fusion* **27** (1987) 867.
- [8] STROTH, U., et al., *Nucl. Fusion* **36** (1996) 11.
- [9] SUDO, S., et al., *Nucl. Fusion* **30** (199) 1063.
- [10] BEIDLER, C., et al., Fusion Energy 1996, Vol. 3, 407 (IAEA, Vienna 1997).
- [11] YAMAZAKI, K., et al., Fusion Energy 1996, Vol. 3, 421 (IAEA, Vienna 1997).

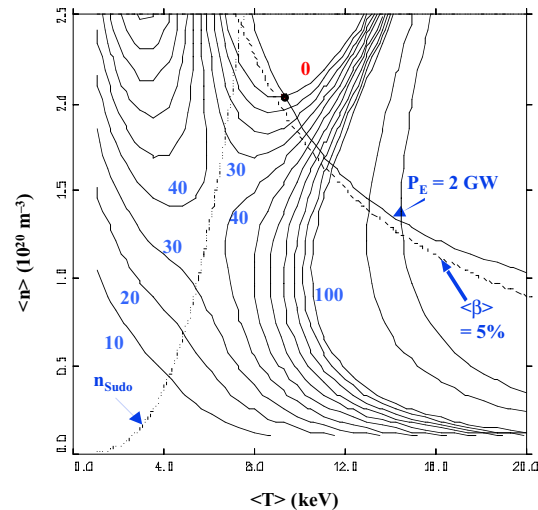


Fig. 7. QP#1 reactor with $P_{\text{electric}} = 2$ GW.